Spin correlation parameter A_{nn} in pp elastic scattering at 796 MeV

M. W. McNaughton,* H. W. Baer,† P. R. Bevington,‡ F. H. Cverna,† H. B. Willard,§ and E. Winkelmann‖
Case Western Reserve University, Cleveland, Ohio 44106

E. P. Chamberlin, J. J. Jarmer, N. S. P. King, and J. E. Simmons
Los Alamos Scientific Laboratory, Los Alamos, New Mexico 87545

M. A. Schardt
Arizona State University, Tempe, Arizona 85281

H. Willmes
University of Idaho, Moscow, Idaho 83843

(Received 4 August 1980)

The spin correlation parameter $A_{nn}(\theta)$ for pp elastic scattering has been measured at 796 MeV from 30° to 90° c.m. The typical relative uncertainties of ±0.01 are almost an order of magnitude better than those of previous data near this energy. The absolute normalization uncertainty is ±2%. Data are consistent with previous measurements near this energy.

[NUCLEAR REACTIONS ^{1}H(p,p)^{1}H, E=796 MeV; measured $A_{nn}(\theta)$, $A(\theta)$; θ=30 to 90° c.m.]

I. INTRODUCTION

As part of our program to determine the $I=1$ nucleon-nucleon amplitudes near 800 MeV, we have measured the spin correlation parameter $A_{nn}(\theta)$ for pp elastic scattering from $\theta=30°$ to 90° c.m. This parameter, also written as A_{yy}, C_{nn}, or (NN00),[1] is further defined below. The present 796 MeV data do not differ significantly from the preliminary data presented previously,[2] but analysis of the 643 MeV data is not complete, and the earlier values[2] should be considered preliminary.

These measurements, together with previous measurements by this group, of the differential cross section[3] and analyzing power[4,5] have significantly constrained the phase shift analysis near 800 MeV.[6] Phase shift fits to the data are shown in Fig. 1.

It is well known that at least nine independent parameters are required for an unconstrained analysis of the $pp \to pp$ amplitudes above pion production threshold. In addition to the data listed above, there are data for C_{LL} near 800 MeV.[7] Preliminary data for six further parameters (D_{NN}, D_{SS}, D_{LS}, K_{NN}, K_{SS}, and K_{LS}, bringing the total to ten) are presented in Ref. 8. These data should provide a solution near 800 MeV for the $I=1$ amplitudes that will clarify the interpretation of the resonancelike structure observed near 800 MeV.[7,9] These data at 800 MeV are also urgently needed for the interpretation of proton-nucleus data. It has been stated[10] that the "imprecise (nucleon-nucleon) data have become the principal obstruction to the analysis of the new LAMPF and Saclay (proton-nucleus) data." This is discussed in more detail in Ref. 11.

Previous measurements of A_{nn} near this energy are shown in Fig. 2. Earlier data are tabulated in Ref. 12. New data from the zero-gradient synchrotron (ZGS) (Refs. 13–15) interpolate to values consistent with the data presented here. New data at lower energies from SIN (Refs. 16 and 17) are also shown in Fig. 2.

The measurement of the initial state spin correlation parameter A_{nn} involves scattering a beam of polarized protons from a polarized proton target and measuring the difference in yield for spins parallel and antiparallel. The basic formula is

$$\sigma(\uparrow\uparrow) = \sigma(1 + P_t A + P_b A + P_t P_b A_{nn}), \quad (1)$$

where $\sigma(\uparrow\uparrow)$ and σ are spin-dependent and spin-

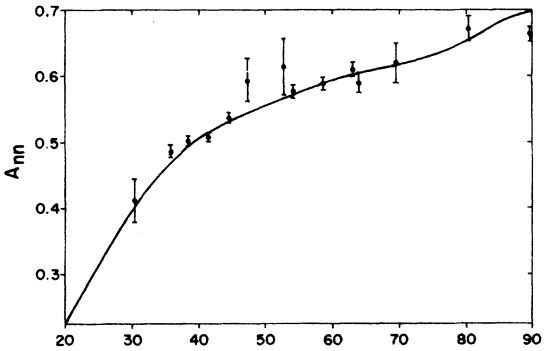

FIG. 1. Spin correlation parameter $A_{nn}(\theta)$ for $pp \to pp$ at 796 MeV compared with a recent phase shift fit (CD79) (Ref. 6).

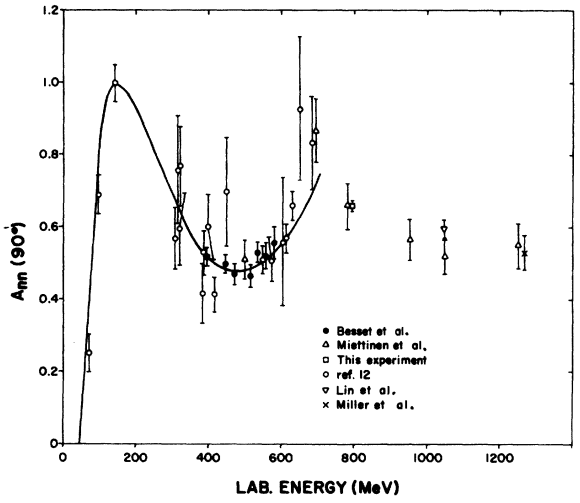

FIG. 2. A_{nn} (90°) vs incident lab energy (adapted from Ref. 17) comparing present with previous data (Refs. 12–17). The curve is the Saclay phase shift fit.

averaged yields, P_t and P_b are target and beam polarization, and A is the analyzing power. The spin correlation parameter A_{nn} is then given by

$$A_{nn}=\frac{1}{P_b P_t}\frac{\sigma(\uparrow\uparrow)+\sigma(\downarrow\downarrow)-\sigma(\uparrow\downarrow)-\sigma(\downarrow\uparrow)}{\sigma(\uparrow\uparrow)+\sigma(\downarrow\downarrow)+\sigma(\uparrow\downarrow)+\sigma(\downarrow\uparrow)}. \quad (2)$$

II. EXPERIMENTAL METHOD

The experimental apparatus is sketched in Fig. 3. A beam of polarized protons was obtained from the LAMPF accelerator. Typical beam parameters were ≤1 pA intensity, ~5 mm diameter spot size, and beam polarization $P_b \simeq 0.9$.

Intensity fluctuations between beam and target reversals were monitored to about one percent accuracy by the combination of an ion chamber,[18] and by the sums of yields (left plus right, and up plus down) of the beam line polarimeter. Spot size and position were monitored to 1 mm with a beam profile monitor.[19] Beam polarization was measured to better than 1% simultaneously with every data run by the extended proton beam (EPB) beam line polarimeter.[20]

The beam was directed onto a conventional ^{3}He-propanediol polarized target (see Sec. III) and the

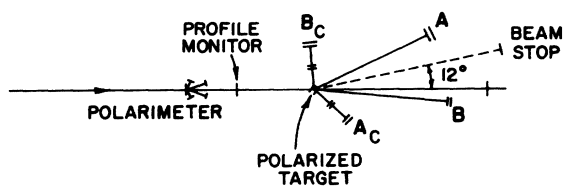

FIG. 3. Experimental layout: $(A\cdot A_c)$ and $(B\cdot B_c)$ are MWPC arms in coincidence for left and right scattering.

scattered protons detected in multi-wire proportional chambers[21] (MWPC's) arranged in four arms. In a typical setup, a proton scattering left was detected in coincidence with its conjugate recoil proton in the detector arms $A\cdot A_c$, while a proton scattering right was detected along with its conjugate proton in the detectors $B\cdot B_c$. Simultaneous use of pairs A and B set at equal angles to the left and right allowed cancellation of instrumental asymmetries in a manner analogous to the method commonly used for analyzing power measurements.[22] Backward of 27.4° lab it was impossible (mechanically) to set both A and B arms at the same angle, so data were taken with the A arm alone at $\theta \geq 27.4°$ lab. For these measurements, the B arm was set near 17.5° lab to monitor the target polarization, allowing an independent check of the measurement from the NMR system (Sec. IV). These two method of measurement agreed to within 1%.

Data for every event were monitored on-line and recorded for subsequent off-line analysis. If a single particle fired two or more adjacent MWPC wires, the centroid of the clump was recorded. If more than one particle traversed an MWPC, the centroids of the first two clumps were recorded. The majority of such double tracks were from knock on electrons (δ rays), which are a constant fraction (about 7%) of all events. It was found that these multiple tracks could be included or excluded without significantly affecting the result. Because of the better cancellation of systematic errors in the analysis of data where $\theta_A = \theta_B$ (see Sec. V) multiple tracks were excluded in the final analysis of data when $\theta_A = \theta_B$, but included when $\theta_A \neq \theta_B$.

Detector (MWPC) dead time was determined by scaling a beam monitor (the polarimeter "up" coincidence) both alone and in coincidence with the MWPC busy signal. As with multiple tracks, it was found best to include this correction when $\theta_A \neq \theta_B$ and exclude it when $\theta_A = \theta_B$. Agreement between results in the two cases assured us that these corrections were being handled correctly.

Target "empty" data were obtained in separate runs by removing the propanediol ($C_3H_8O_2$) target material from the target cavity and substituting graphite of approximately equal mass and volume. Comparison was made between the results after subtracting these data and simulated data generated by a Monte Carlo calculation; no significant difference was observed. In general, true target empty data were used to obtain the final results.

The beam polarization was reversed about every two hours. Data were (in general) arranged in cycles of four runs with target spins successively ↑↓↓↑ to minimize systematic errors. Typ-

ically, two cycles (four ↑↓ pairs) were taken at each angle.

III. POLARIZED PROTON TARGET

The polarized proton target was developed at the Los Alamos Scientific Laboratory, and is based on well-known technology.[23] It consisted, in principle, of beads (≃1 mm diameter) of propanediol ($C_3H_8O_2$) doped with ≃2% by weight of Cr(V) immersed in a bath of liquid ^{3}He. The target material was packed into a right cylinder of teflon (≤100 μm thick, 19 mm long, 19 mm diameter), which in turn was contained within the copper microwave cavity (100 μm thick), the stainless steel ^{3}He gas container (250 μm thick), a heat shield (250 μm aluminum), and vacuum jacket (380 μm stainless steel).

A uniform (1 in 10^4) vertical magnetic field of 2.5 T was provided by a conventional C magnet that allowed unrestricted scattering through most of the horizontal plane. Other materials such as NMR coils, microwave guides, and thermometry were located near the target. Care was taken, however, to exclude unpolarized hydrogen from the target cavity, and to keep the configuration similar between target full and empty runs.

The target was dynamically polarized by bombardment with a few mW of 70 GHz microwave power. Typical target polarization was about 0.83. By increasing the microwave power to ~50 mW and changing the microwave frequency by about 0.5%, the direction of polarization could be reversed in about 20 to 30 min.

Further details of the construction, performance, and operation of the polarized target are contained in an informal report that may be obtained from the authors.

IV. POLARIZED TARGET NMR

The target polarization was monitored by a conventional Q-meter NMR system. Two NMR coils were placed in the vicinity of the target and connected by one-wavelength coaxial cables to a parallel resonance circuit. The LC resonance shape (and some coherent noise) was subtracted by feeding one input of a differential amplifier with the NMR signal and the second with a dummy signal, identical with the first except for the absence of target material (and therefore NMR) near the coil. The NMR signal was monitored visually during data runs, and recorded at the beginning and end of a run. Often a few percent increase in polarization was observed during the run, and an appropriate average was taken.

Absolute calibration of the NMR signal was obtained by comparison with thermal equilibrium signals. A typical thermal equilibrium signal (average of 256 sweeps) is shown in Fig. 4. Measurements were made on 13 separate days, recording 10 to 50 spectra of typically 256 sweeps each time. In general, the results were internally consistent to within 2%.

The subtraction of the LC resonance curve obtained by the dummy circuit was adequate for the large polarized signal, but was never sufficiently well tuned to be adequate for the thermal equilibrium signal. Consequently, a further subtraction of the small residual LC shape was made by changing the magnetic field sufficiently to get rid of the NMR signal. The magnetic field was alternately raised and lowered by about 1% in order to avoid relaxation to a time averaged field different from the standard field. On some occasions a significant difference of a few percent was observed between the results with the field raised and lowered. This was subsequently understood as resulting from a "ghost" signal from frost on the NMR cable outside the target cavity about 5 cm from the target. Since this hydrogen was in a higher field than the central field, its influence was only felt when the central field was lowered by ≥1%. Comparison of the results from raised and lowered fields, and correction where necessary, convinces us that the errors from this problem are small (≃1%)

A number of other systematic errors are possible and have been carefully considered. It is well known that the large size of the NMR signal relative to the rf carrier leads to an apparent difference between the measurements for the two polarization directions. We applied the corrections recommended by Hill and Hill[24] with generally good results. The inclusion of the two arms (A and B, see Sec. II) allowed us

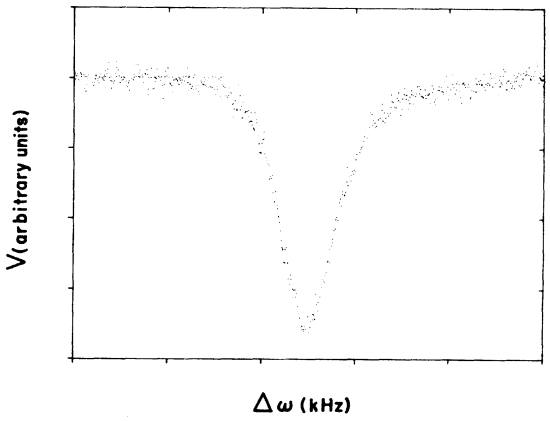

FIG. 4. Typical NMR signal for thermal equilibrium conditions (averaged over 256 sweeps).

a variety of cross checks on this problem (see Sec. V). In almost all cases, the indications from the NMR and the scattering data agreed, and we conclude that in 90% of the runs there was no significant (2%) difference between the absolute magnitudes in the two directions. In the remaining cases where the polarization difference was apparently real, the appropriate corrections were made (see Sec. V).

The region of the target sampled by the NMR coil is, in general, different from the region sampled by the beam, so that nonuniform target polarization would lead to a systematic error. Although we included two NMR coils to sample two different regions of the target, at no time during these data runs did we have both coils working simultaneously. We have subsequently had both coils working simultaneously, and observed $\leq 2\%$ difference between them on all occasions. Furthermore, the excellent agreement between the measurements from NMR and independent measurements of target polarization from scattering assure us that this is not a significant problem.

We estimate the maximum radiation dose received by one batch of target material to be about 10^{12} protons/cm^2. No significant (1%) radiation damage was observed, which is consistent with Ref. 25.

This was the first experiment performed with the polarized target and a variety of problems were encountered resulting in several changes of target material and several changes in the NMR setup. The 13 days on which calibrations were taken correspond to eight different sets of conditions. The agreement between these data is reassuring.

In summary, we have assigned an uncertainty of ± 0.02 to the NMR measurement of target polarization for most individual runs, increasing this value as appropriate for certain runs, e.g., when the separate NMR measurements for one run differed significantly. We have assigned a further 2% uncertainty, applicable to all data equally, to cover possible systematic error in our absolute calibration (see Sec. VI).

V. DATA ANALYSIS

The data tapes recorded on-line were analyzed off-line to obtain the pp elastic scattering yields for each spin combination at each angle. The MWPC data from the primary and conjugate detector arms were used to obtain a target traceback (to exclude events that did not originate in the target) and to obtain angular correlation between primary and conjugate protons. In the absence of Coulomb multiple scattering, finite detector resolution, and similar broadening effects, the angular correlation should be a delta function both in the horizontal (opening angle) and the vertical (coplanarity). A typical angular correlation spectrum is shown in Fig. 5. The hydrogen peak is seen clearly on a background of events from quasi-free scattering [e.g., $C(p,2p)$] and random coincidences.

At forward angles ($\leq 12.5°$ lab) multiple Coulomb scattering broadened the angular correlation peak to the extent that pp elastic scattering events were almost indistinguishable from $C(p,2p)$ quasi-elastic events. This experimental problem limited the extreme forward angle at which data could be taken, and is the primary cause of the large uncertainty on the 12.5° lab point.

Target empty (i.e., hydrogen free) data were obtained as mentioned in Sec. II. Because of the uncertainty in the amount of target material in the beam, normalization between target "full" and empty was made by reference to the wings of the spectra. Typically background was about 10% of the peak. The uncertainty in background subtraction was estimated to be about 10% of the background or 1% of the yield.

The yields for pp elastic scattering were used to calculate the final results in a variety of ways with many cross checks, as follows. The basic formula is Eq. (1) (and similarly for the other spin combinations). We have mentioned (Sec. IV) the possibility that the target polarization might differ in magnitude after reversal. We therefore write the two target polarizations $(P_t+\delta)$ for spin up and $-(P_t-\delta)$ for spin down. Similarly, we write $(P_b+\epsilon)$ and $-(P_b-\epsilon)$ for the beam polarizations. In addition, because of the long time (2 h) between target reversals,

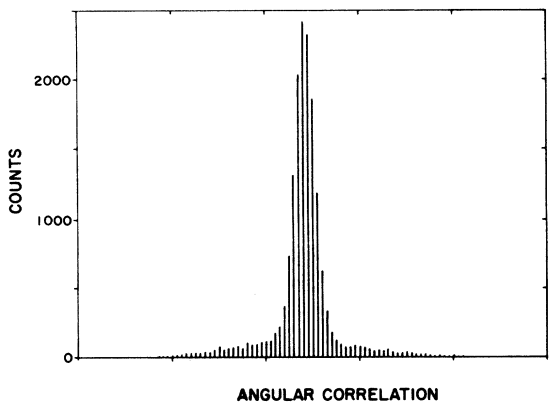

FIG. 5. Angular correlation between primary and conjugate scattered protons in $pp \to pp$.

we found it necessary on a few occasions to write the *beam* polarization $\pm(P_b+\gamma)$ for *target* up and $\pm(P_b-\gamma)$ for target down. In practice, γ was determined directly since the beam line polarimeter measured P_b separately for every run, but δ and ϵ were more difficult (see below). We set $\delta=0$ except when the indications from both scattering and NMR agreed (about one run in ten). There was never any clear indication of $\epsilon\neq 0$, so we set $\epsilon=0$ through the final analysis.

Because of the necessity of distinguishing between target up and beam up, we write U and D for target up and down, and N and R for the two beam spin directions, known as "normal" and "reverse." We then combine the four equations similar to (1) as follows:

$$\mathrm{NU}-\mathrm{ND}-\mathrm{RU}+\mathrm{RD}=E_1=K(P_bP_tA_{nn}+\gamma A), \tag{3}$$

$$\mathrm{NU}-\mathrm{ND}+\mathrm{RU}-\mathrm{RD}=E_2=KP_t(A+\epsilon A_{nn}), \tag{4}$$

$$\mathrm{NU}+\mathrm{ND}-\mathrm{RU}-\mathrm{RD}=E_3=K[P_b(A+\delta A_{nn})+\gamma P_tA_{nn}], \tag{5}$$

$$\mathrm{NU}+\mathrm{ND}+\mathrm{RU}+\mathrm{RD}=E_4=K[1+A(\epsilon+\delta)+\epsilon\delta A_{nn}]. \tag{6}$$

(Note: These are for scattering left. When scattering right, the sign of every term containing the analyzing power A must be changed).

The quantities NU etc., are the yields of good elastic events after background subtraction, normalized to the number of incident beam particles, and corrected for dead time and multiple tracks in the MWPC's. Those experimental quantities that remain constant, such as target thickness, cross section, solid angle, and detector efficiency, are included in the constant K, which cancels from the final equations.

These equations may now be solved (canceling K) to give expressions for A_{nn}, A, P_t, δ, etc., e.g., if $\gamma=\delta=\epsilon=0$, then Eq. (2) is

$$A_{nn}=\frac{1}{P_bP_t}\frac{E_1}{E_4}. \tag{7}$$

Provided $A\neq 0$, we also have

$$P_t=P_b\frac{E_2}{E_3}. \tag{8}$$

When the two arms (A and B) are at equal angles, there are eight equations similar to Eq. (1) with eight yields for which we write ANU (for A arm, beam normal, target up), BNU, etc. Because of the better cancellation of experimental quantities in the analysis of the data with $\theta_A=\theta_B$, the quantities ANU, etc., were not corrected for incident beam, dead time, or multiple tracks.

In the case $\gamma=\delta=\epsilon=0$, then only seven of these equations are independent. This follows from the identity

$$\frac{(\mathrm{ANU})\,(\mathrm{ARD})\,(\mathrm{BND})\,(\mathrm{BRU})}{(\mathrm{BNU})\,(\mathrm{BRD})\,(\mathrm{AND})\,(\mathrm{ARU})}=1, \tag{9}$$

which provides a prescription for deriving any equation from the other seven. The ratio of products in Eq. (9) differs from unity only if a number has been incorrectly entered or if γ, δ, or $\epsilon\neq 0$, so Eq. (9) is a useful check.

The eight yields from two arms at equal angles are most conveniently handled by defining

$$r^2=\frac{(\mathrm{ANU})\,(\mathrm{BRD})}{(\mathrm{BNU})\,(\mathrm{ARD})}, \tag{10}$$

$$s^2=\frac{(\mathrm{ARU})\,(\mathrm{BND})}{(\mathrm{BRU})\,(\mathrm{AND})}, \tag{11}$$

$$R=\frac{r+1}{r-1}, \tag{12}$$

$$S=\frac{1+s}{1-s}, \tag{13}$$

$$A_{nn}=\frac{1}{P_bP_t}[A(P_b+P_t)R-1], \tag{14}$$

$$P_t=\frac{2-P_bA(R+S)}{A(R-S)}. \tag{15}$$

Equations (14) and (15) are independent provided $P_t\neq P_b$. Unfortunately, as (P_b-P_t) approaches zero, Eq. (15) degenerates. Furthermore, Eq. (14) requires the analyzing power A to be accurately known. Advantages of Eqs. (14) and (15) are

(i) γ, δ, ϵ disappear to order γ^2, δ^2, ϵ^2.

(ii) The number of beam particles and number of target particles cancel from Eqs. (10)–(15), but not from Eqs. (3)–(8).

The calculation of uncertainties for the above formulas involves straightforward but tedious algebra. A full list of relevant formulas with their uncertainties may be obtained from the authors.

For every run, all possible quantities were calculated in a variety of ways to take full advantage of all consistency checks. When all methods were consistent, the following sequence was followed to obtain the final result. First, P_t and δ were determined from both NMR and scattering, and a weighted mean taken. When two arms were at equal angles, Eq. (15) was used. Otherwise, the B arm was set near 17.5° lab and Eq. (8) was used. Uncertainties were typically about ±0.02 for both NMR and scattering determinations. Finally, substitution into Eq. (7) or (14) gave A_{nn}.

Values were also obtained for the analyzing power A by averaging over target spin

$$A=\frac{1}{P_b}\frac{E_3}{E_4}. \tag{16}$$

VI. DISCUSSION OF RESULTS

Data are tabulated in Table I for both the spin correlation parameter A_{nn} and for the analyzing power A. The analyzing power results are in general in agreement with, but less accurate than those from Refs. (4) and (5).

The nonzero value of the analyzing power near 90° c.m. indicates an error of about 0.4° lab in the intended detector settings for these data. Since the A_{nn} function is flat near 90° c.m. this error is insignificant. The uncertainty in the angular setting is estimated to be about ±0.3° lab; the uncertainty resulted from the difficulty of calculating the bend in the magnetic field given the uncertainties in the precise starting location, and the uncertainty in energy loss of protons emerging from the target.

The measured value of the analyzing power at 22.4° lab is anomalously high. We believe it unlikely that the detectors were misaligned by several degrees as would be required to explain this discrepancy. We are unable to explain this anomaly, but we have increased the uncertainty on this point. Specifically, use of $A = 0.481$ (from Ref. 2) in Eq. (14) gives $A_{nn} = 0.568 \pm 0.016$, while $A = 0.501$ (from Table I) gives $A_{nn} = 0.652 \pm 0.02$. The tabulated value represents the mean and spread of these two values. The same problem (but less severe) exists with the 20° lab point (measured on the same day as the 22.4° point) with $A_{nn} = 0.574 \pm 0.037$ corresponding to the presently measured value of A, and $A_{nn} = 0.608 \pm 0.028$ corresponding to the previously published value.[2] The smaller uncertainties for the 18.8° and 23.0° lab points make the problem somewhat moot.

TABLE I. Analyzing power A and spin correlation parameter A_{nn} for pp elastic scattering at 796 MeV. Note that an overall normalization uncertainty of ±2% should be applied to all A_{nn} data simultaneously (see Sec. IV).

θ_{lab}	$\theta_{c.m.}$	A	Δ_A	A_{nn}	ΔA_{nn}
12.8	30.3	0.463	0.009	0.407	0.034
15.1	35.7	0.490	0.006	0.483	0.009
16.2	38.2	0.495	0.005	0.498	0.007
17.5	41.2	0.492	0.004	0.504	0.005
18.8	44.2	0.491	0.006	0.534	0.007
20.0	47.0	0.507	0.013	0.591	0.032
22.4	52.4	0.501	0.005	0.611	0.043
23.0	53.7	0.475	0.006	0.574	0.010
25.0	58.2	0.459	0.005	0.586	0.009
27.0	62.6	0.418	0.007	0.608	0.010
27.4	63.5	0.419	0.045	0.587	0.015
30.0	69.1	0.331	0.040	0.617	0.030
35.0	79.8	0.271	0.071	0.669	0.019
39.6	89.3	0.020	0.008	0.661	0.010

The measurement near 90° c.m. includes data taken with the A arm, using the B arm as monitor of P_t, and data taken with the B arm with only the NMR to monitor P_t. Results at 17.5° lab include data from single arm ($\theta_B = 17.5°$) as well as double arm ($\theta_A = \theta_B = 17.5°$) measurements All results are consistent for both these angles.

A decrease in the efficiency of one MWPC detector affected the 27.4°, 30°, and 35° lab data to a small extent. The over determination of this experiment allowed these data to be improved by assuming that the efficiency was changing as a smooth function of time and adjusting an efficiency factor to optimize the internal consistency. The values before adjustment were $A_{nn} = 0.583$, 0.593, and 0.675, respectively, yielding changes of 0.3, 1, and −0.3 standard deviations.

A weighted average was obtained over all runs for the ratio of the values of P_t from NMR, and P_t from scattering [Eq. (8) or (15)]. The result is

$$\frac{P_t(\text{scatter})}{P_t(\text{NMR})} = 1.002 \pm 0.005.$$

The quoted uncertainty represents internal errors only, without the overall 2% normalization uncertainty suggested below. Since the equations for P_t(scatter) include P_b, the comparison is essentially between the quench ratio calibration of the beam polarization[4,5] and the thermal equilibrium calibration of the NMR.

In general, the uncertainties calculated for individual runs were consistent with the dispersion of individual runs about the mean. The exceptions (20°, 22.4°, 30°, and 35° lab), for which the uncertainties have been increased to take a account of anomalous dispersion, have been discussed above.

Typical contributions to the overall uncertainty at one angle are as follows:

target polarization	1.3%
counting statistics	1%
beam polarization	0.8%
beam intensity	0.7%
dead time	0.5%
background subtraction	0.5%
Total	2%

These uncertainties (as quoted in Table I) are relative point to point only. The absolute normalization of both beam and target polarization are to some extent inter-related. We recommend adding a further 2% (in quadrature) to represent the common normalization uncertainty, i.e., all data are

subject to a common normalization factor of 1.00 ± 0.02.

ACKNOWLEDGMENTS

We wish to thank Jan Boissevain and Charles Newsome for assistance with the polarized target, Kok-Heong McNaughton for assistance with the analysis, Gloria Garcia and Gary French for their assistance preparing the paper, and the staff of LAMPF for their assistance and cooperation throughout all phases of the experiment. This work was supported in part by the Department of Energy.

---

*Present address: MS-838, Los Alamos Scientific Laboratory, Los Alamos, N. M. 87545.

†Present address: Los Alamos Scientific Laboratory, Los Alamos, N. M. 87545.

‡Deceased, August 19, 1980.

§Present address: National Science Foundation, Washington, D. C. 20550.

¶Present address: Physik Inst. der Univ. Zurich, Switzerland.

[1]The notation A_{mn} follows the Ann Arbor convention as recommended in *Higher Energy Polarized Beams (Ann Arbor, 1977)*, Proceedings of the Workshop on Higher Energy Polarized Proton Beams, edited by A. D. Krisch and A. J. Salthouse (AIP, New York, 1978), p. 142.

[2]M. W. McNaughton *et al.*, presented at the Washington meeting of the APS (April 24–27, 1978); H. B. Willard *et al.*, *High Energy Physics with Polarized Beams and Polarized Targets (Argonne, 1978)*, Proceedings of the Third International Symposium on High Energy Physics with Polarized Beams and Polarized Targets, edited by G. H. Thomas (AIP, New York, 1979), p. 420.

[3]H. B. Willard *et al.*, Phys. Rev. C 14, 1545 (1976).

[4]P. R. Bevington *et al.*, Phys. Rev. Lett. 41, 384 (1978).

[5]M. W. McNaughton *et al.*, Phys. Rev. C (to be published).

[6]R. A. Arndt and L. D. Roper (unpublished).

[7]I. P. Auer *et al.*, Phys. Rev. Lett. 41, 1436 (1978).

[8]M. W. McNaughton *et al.*, submitted to the Fifth International Symposium on Polarization, Santa Fe, New Mexico (1980).

[9]W. de Boer *et al.*, Phys. Rev. Lett. 34, 558 (1975); E. K. Biegert *et al.*, Phys. Lett. 73B, 235 (1978); I. P. Auer *et al.*, *ibid.* 67B, 113 (1977); 70B, 475 (1977); H. Hidaka *et al.*, *ibid.* 70B, 479 (1977); I. P. Auer *et al.*, Phys. Rev. Lett. 41, 354 (1978).

[10]Los Alamos Scientific Laboratory Report No. LA-8335C 1980, Vol. I (unpublished), p. 66.

[11]L. Ray, Phys. Rev. C 19, 1855 (1979).

[12]J. Bystricky, F. Lehar, and Z. Janout, Saclay Report No. CEA-N-1547, 1972 (unpublished).

[13]K. Abe *et al.*, Phys. Lett. 63B, 239 (1976); H. E. Miettinen *et al.*, Phys. Rev. D 16, 549 (1977); J. R. O'Fallon *et al.*, Phys. Rev. Lett. 39, 733 (1977); M. Borghini *et al.*, Phys. Rev. D 17, 24 (1978); A. Lin *et al.*, Phys. Lett. 74B, 273 (1978); D. G. Crabb *et al.*, Phys. Rev. Lett. 43, 983 (1979); E. A. Crosbie *et al.*, University of Michigan Report No. UM-HE-80-2, 1980 (unpublished).

[14]T. A. Mulera, *High Energy Physics with Polarized Beams and Polarized Targets (Argonne, 1978)*, Proceedings of the Third International Symposium on High Energy Physics with Polarized Beams and Polarized Targets, edited by G. H. Thomas (AIP, New York, 1979), p. 428; H. E. Miettinen *et al.*, presented at the Washington meeting of APS (1980); D. A. Bell *et al.*, Phys. Lett. 94B, 310 (1980).

[15]D. M. Miller *et al.*, Phys. Rev. Lett. 36, 763 (1976); D. Miller *et al.*, Phys. Rev. D 16, 2016 (1977).

[16]D. Besset *et al.*, *High Energy Physics with Polarized Beams and Polarized Targets (Argonne, 1978)*, Proceedings of the Third International Symposium on High Energy Physics with Polarized Beams and Polarized Targets, edited by G. H. Thomas (AIP, New York, 1979), p. 424.

[17]D. Besset *et al.*, Nucl. Phys. A345, 435 (1980).

[18]R. J. Barrett *et al.*, Nucl. Instrum. 129, 441 (1975).

[19]G. J. Krausse and P. A. M. Gram, Los Alamos Scientific Laboratory Report No. LA-7142, 1978 (unpublished).

[20]M. W. McNaughton, Los Alamos Scientific Laboratory Report No. LA-8307-MS, 1980 (unpublished).

[21]P. R. Bevington and R. A. Leskovec, Nucl. Instrum. 147, 431 (1977).

[22]G. G. Ohlsen and P. W. Keaton, Nucl. Instrum. 109, 41 (1973).

[23]*Proceedings of the Second International Conference on Polarized Targets*, edited by G. Shapiro (Univ. of California Press, Berkeley, 1971).

[24]J. J. Hill and D. A. Hill, Argonne National Laboratory Report No. ANL/HEP-7359, 1973 (unpublished).

[25]R. Fernow, Nucl. Instrum. 148, 311 (1978).